Journal of Physics: Conference Series **712** (2016) 012076 doi:10.1088/1742-6596/712/1/012076

XAFS study on a photodeposition process of Pt nanoparticles on TiO_2 photocatalyst

T. Yoshida*[1,2], Y. Minoura[3], Y. Nakano[3], M. Yamamoto[3], S. Yagi[1], H. Yoshida[4,5]
[1]EcoTopia Science Institute, Nagoya University, Nagoya 464-8603, Japan,
[2]The OCU Advanced Research Institute for Natural Science and Technology, Osaka City University, Osaka 558-8585, Japan
[3]Graduate School of Engineering, Nagoya University, Nagoya 464-8603, Japan,
[4]Kyoto University, Graduate School of Human and Environmental Studies, Kyoto 606–8501, Japan
[5]Elements Strategy Initiative for Catalysts and Batteries, Kyoto University, Kyoto, 606-8501, Japan

E-mail: tyoshida@ocarina.osaka-cu.ac.jp

Abstract. A photodeposition process of Pt metal particles on anatase TiO_2 in the aqueous solution of H_2PtCl_6 (precursor) and methanol (reductant) was studied using transmission electron microscopy, UV-vis spectroscopy and X-ray absorption fine structure spectroscopy. These analyses proposed the photodeposition mechanism of Pt on TiO_2 by the photogenerated electrons: the photo-assisted adsorption of Pt^{4+} complexes on TiO_2 through the ligand exchange at the initial stage, followed by the successive rapid reduction of Pt^{4+} to Pt^0 to grow the Pt metal particles, which gives small and almost uniform size of Pt metal nanoparticles.

1. Introduction

Photoreduction is one of the most popular methods for recovering noble metals, removing metal cations from aqueous effluents and preparing metal-loaded photocatalysts [1-5]. The UV irradiation on a semiconductor material such as TiO_2 photocatalyst can form photoexcited electrons on the surface, which can reduce some kinds of metal cations having appropriate redox potential to produce metal particles on the surface. The interaction between the semiconductor and the metal could play an important role for the photocatalytic activity, since the support-metal junction could influence the electronic properties of them, the electron transfer between them and the morphology of the metal particles [6,7]. However, there are only a few studies dealing with the mechanism of the photodeposition process and the structure of the photodeposited metal species [8-10].

Recently, Ohyama *et al.*[8] studied the photodeposition process of Rh metal particles on TiO_2 using in situ time-resolved energy dispersive X-ray absorption fine structure spectroscopy (DXAFS) and reported that the $RuCl_3$ precursor was reduced to form Rh metal particles where the coordination number of the reduced Rh atom increased proportionally with the photoirradiation time, suggesting that fine Rh metal particles with uniform size appeared one after another. In the present study, we examined the photodeposition processes of Pt metal particles on anatase TiO_2 by means of XAFS, together with UV-vis spectroscopy and transmission electron microscopy.

2. Experimental

Photodeposition of Pt metal particles on TiO_2 was carried out as follows: $H_2PtCl_6 \cdot 6H_2O$ powder of 13.4 mg was dissolved in a methanol aqueous solution of 60 mL (the mixture of 50 mL of distilled water and 10 mL of methanol). 1.0 g of an anatase TiO_2 sample (Kishida Kagaku Co., BET surface area was 5.3 m^2/g) calcined at 673 K in air was suspended in the aqueous solution of the Pt precursor. The suspension was irradiated for various periods (0–180 min) with a 300 W Xe lamp equipped with a band path filter (ca. 340±30 nm, 30 mW/cm^2), and then filtered and washed with purified water.
UV-vis diffuse reflectance spectra were measured by a JASCO V-670 spectrometer. TEM images were obtained with a JEOL JEM-2100M transmission electron microscope operating at an accelerating voltage of 200 kV. TEM samples were prepared by depositing drops of methanol suspension containing small amounts of the sample powders onto a carbon-coated copper grid and allowing the methanol to evaporate in air. The XAFS measurements at the Pt L_3-edge were carried out at BL-9C [11] of the Photon Factory at the High Energy Accelerator Research Organization (KEK, Tsukuba Japan, proposal number 2011G575 and 2014G548) with a Si(111) double-crystal monochromator in the fluorescence mode by using a Lytle detector filled with an Ar(100%) flow with a Ga filter ($\mu t = 6$). Ion chamber of the I_0 detector was filled with a N_2(85%)/Ar(15%) flow. The above UV-vis, TEM and XAFS measurements were conducted ex-situ for the Pt species deposited/adsorbed on TiO_2 samples.

3. Results and discussion

Difference UV-vis spectra of the Pt/TiO_2 samples are shown in Figure 1. The difference spectrum of each sample was obtained by subtracting UV-vis spectrum of the pristine TiO_2 sample. As shown in Figure 1, the spectra of the Pt/TiO_2 samples prepared by photodeposition for 5, 10, 15 min showed a band around 400 nm, which would be attributed to the Pt precursors and possibly increasing Pt metallic clusters on the TiO_2 surface. Note that the band became broader and flat feature for the Pt/TiO_2 samples prepared by photodeposition for 20 min, which would originate from metal nanoparticles. This means that the aggregation of Pt atoms occurred under photoirradiation. After that, the band intensity increased with the further photoirradiation whereas the flat spectral profile did not change. These results suggest that the number or the particles size of the Pt nanoparticles on the surface increased with photoirradiation time.

The size of the Pt nanoparticles was observed by TEM measurements. Although the Pt particles were not observed in the Pt/TiO_2 samples prepared by photodeposition for less than 20 min, the Pt nanoparticles were observed and the average size increased from ca. 3.3 to 4 nm with the increase of the photoirradiation time more than 25 min as shown in Figure 2. As mentioned, the absorbance clearly became large as shown in Figure 1, though the size did not varied so drastically as shown in Figure 2. These results suggest that the number of the Pt nanoparticles with similar size of ca. 3–4 nm increased during the photoirradiation after 20 min.

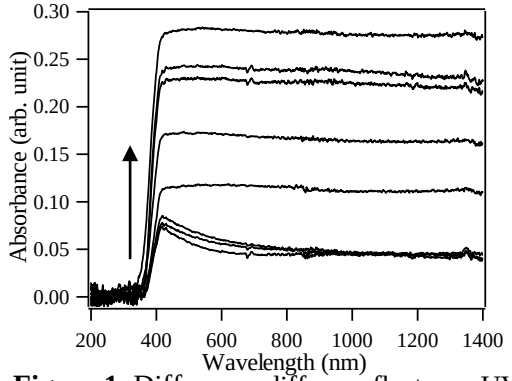

Figure 1. Difference diffuse reflectance UV-Vis spectra of a series of Pt species on TiO_2 by photodeposition for 5, 10, 15, 20, 25, 30, 60 and 180 minutes.

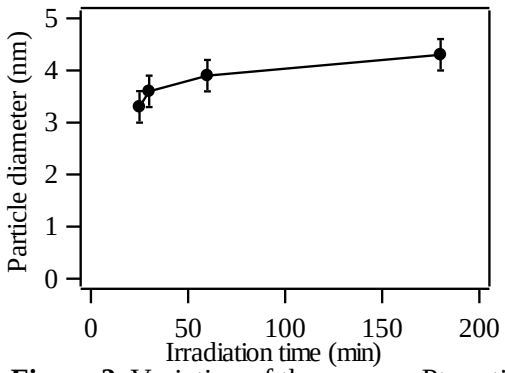

Figure 2. Variation of the average Pt particle size with photoirradiation time. The sizes were obtained from TEM images.

We also investigated the photodeposition process of the Pt metal nanoparticles by XAFS spectroscopy. Figure 3(A) shows normalized Pt L_3-edge XANES spectra of the Pt/TiO_2 samples together with Pt foil and PtO_2 as references. Note that these XANES spectra were normalized by the jump of Pt L_3-edge, i.e., normalized by a Pt atom on the TiO_2 surface. The sharp and narrow absorption band at an absorption edge, which is called white line [12], corresponds to the electronic transition from $2p_{3/2}$ core level states to 6s and 5d orbitals of Pt atoms mainly. The large area of L_3 edge absorption around 11565 eV for PtO_2 results from the vacancy in the 5d orbital of Pt atoms. As shown in Figure 3(A), the feature of XANES spectrum of the TiO_2 sample adsorbing the Pt precursor before photoirradiation was almost similar to that of the reference PtO_2 sample, meaning that the adsorbed Pt species also had similar octahedral structure as PtO_2. Only the difference between the two spectra was the very small peak around 11.545 keV, which is assignable to L_2 edge absorption (11.54 keV) of tungsten as an impurity in the TiO_2 support. The small peak was clearly observed for the Pt/TiO_2 samples prepared by the photodeposition for 0, 5, 10 and 15 min, suggesting that the amount of Pt^{4+} precursors stabilized on TiO_2 surface were still small in the initial stage of the photodeposition.

The energy position of the main peak of XANES shifted to lower X-ray energy with the elongation of photoirradiation time, indicating a decrease in the ratio of Pt^{4+} ions by reduction. Figure 3(B) shows the variation of the spectral shape in this process, where the XANES spectra changed from that of Pt^{4+} ion to that of Pt^0 with an isosbestic point, indicating that Pt^{4+} ions were reduced to Pt^0 without through any stable intermediates. This means that the photoreduction from the adsorbed Pt species to metallic Pt nanoparticles take place drastically.

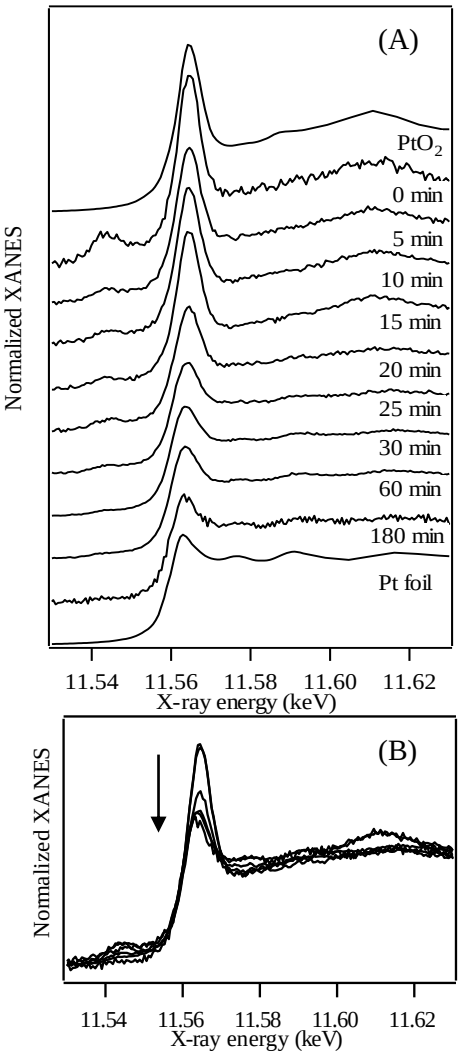

Figure 3. Pt L_3-edge XANES spectra of Pt Pt/TiO_2 samples under photoirradiation for 0, 5, 10, 15, 20, 25, 30, 60 and 180 minutes together with a Pt foil and PtO_2.

Actually, all XANES spectra of the Pt/TiO_2 samples were reproduced with the linear combination of two XANES spectra of PtO_2 and Pt metal, and the fractions of the Pt^{4+} ion and the Pt^0 atom for all the Pt/TiO_2 samples were directly evaluated as shown in Figure 4. Pt^{4+} was the main component in the Pt/TiO_2 samples prepared by photodeposition for 0, 5, 10, and 15 min while the reduction of Pt^{4+} to Pt^0 occurred drastically after 15 min and almost completed after 30 min. Here, we also evaluated the height of edge jump in the raw XAFS spectra of the Pt/TiO_2 samples recorded in the fluorescence mode in order to compare the amount of the Pt species deposited on these samples. Figure 5 shows the variation of the relative height of the edge jump with the photodeposition time. As is evident from Figures 4 and 5, in the initial stage before 15 min, the valence of the adsorbed Pt species was almost tetravalent and the amount of the Pt species increased. It is clear that ca. 20 % of Pt^{4+} complexes were adsorbed on the TiO_2 before photodeposition (0 min) and the Pt^{4+} complexes increased to ca. 50 % by photo-assisted adsorption after 15 min. In the successive period for 20–30 min, the amount of the adsorbed Pt species drastically increased and the reduction of Pt^{4+} to Pt^0 drastically occurred on the photoirradiated TiO_2. After that, the faction of Pt^0 atoms gradually increased by further photoreduction.

These results lead us to speculate the Pt deposition mechanism on the TiO_2 surface. On the whole,

photoexcited electrons reduce the Pt precursor ($[Pt(IV)Cl_6]^{2-} + 4\ e^- \rightarrow Pt(0) + 6\ Cl^-$), while positive holes oxidize methanol in the solution. The details for the photoreduction would be described as follows: (i) during the induction period, the photoexcited electron would stabilize the precursor with ligand-exchange at the surface ($[Pt(IV)Cl_6]^{2-} + \text{-}OH_s^- + e^- + H^+ \rightarrow [Pt(IV)Cl_5O_s]_{ad}^{2-} + Cl^- + H_2$), where the initial amount of the adsorbed Pt complex would be limited by the amount of the surface adsorption sites. (ii) the surface Pt^{4+} complex would be further reduced by the photoexcited electrons to form the Pt metal seeds ($[Pt(IV)Cl_5O_s]_{ad}^{2-} + 3\ e^- \rightarrow Pt(0)O_s + 5\ Cl^-$), and (iii) further photoexcited electrons would drastically reduce the residual Pt^{4+} complexes over the Pt metal seeds to grow itself and to form the Pt metal particles, where the photoexcited electron could be effectively lead to the Pt metallic particles to accelerate the reduction rate of the residual Pt^{4+} complex. The growth of the Pt particles could be limited by the amount of the Pt complexes in the solution.

We have started to investigate the effects of the amount of the Pt precursors and the kind of TiO_2 structural phase on the photodeposition process as well as the morphology of the Pt particles on TiO_2.

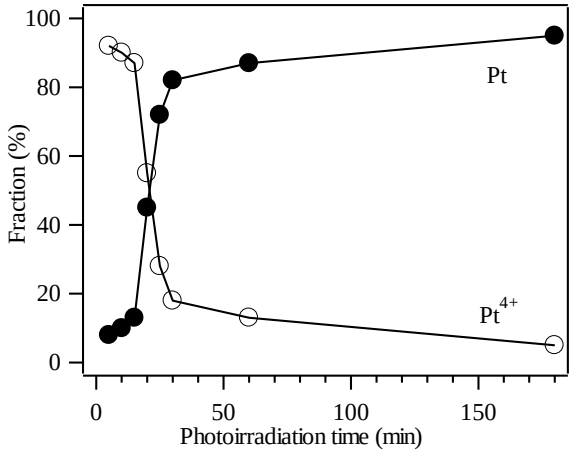

Figure 4. Dependence of the fractions of Pt metal and Pt^{4+} ions on the photoirradiation time.

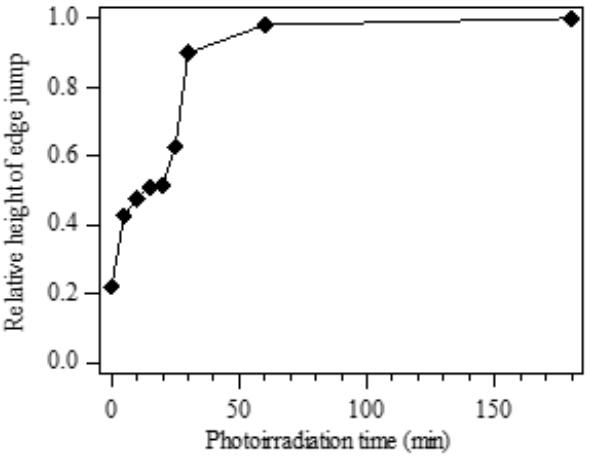

Figure 5. Dependence of the relative height of the edge jump on the photoirradiation time.

4. Conclusion

We studied photodeposition process of Pt particles on an anatase TiO_2 sample. The Pt^{4+} precursors were found to be photo-adsorbed on the TiO_2 surface through ligand exchange at the initial stage. After the formation of the metallic Pt seeds, they were drastically reduced to form the Pt metal particles with almost similar size of 3–4 nm in the present condition.

References

[1] Kraeutler B and Bard A. J, *J. Am. Chem. Soc.* 1977 **99** 7729.
[2] Kraeutler B and Bard A. J *J. Am. Chem. Soc.* 1978 **100** 4317.
[3] Duonghong D, Borgarello E and Graetzel M, *J. Am. Chem. Soc.* 1981 **103** 4685.
[4] Courbon H, Herrmann J M and Pichat P, *J. Phys. Chem.* 1984 **88** 5210.
[5] Goren Z, Willner I, Nelson A J and Frank A J, *J. Phys. Chem.*1990 **94** 3784.
[6] Bond GC 1982 Metal-support and metal-additive effect in catalysis, (Amsterdam, Elsevier) p 1.
[7] Thomson SJ, *J Chem Soc Faraday Trans Part I* **83** 1893.
[8] Ohyama J, Teramura K, Okuoka K, Yamazoe S, Kato K, Shishido T and Tanaka T 2010 *Langmuir* **26** 13907.
[9] Ohyama J, Yamamoto A, Teramura K, Shishido T and Tanaka T, 2011 *ASC Catal.* **1** 187.
[10] Tanaka T, Ohyama J, Teramura T and Hitomi Y, *Catal. Today*, 2012 **183** 108.
[11] http://pfxafs.kek.jp/beamline/bl9c
[12] Brown M, Peiels RE and Stern EA 1977 *Phys Rev B* **15** 738.